Critical Threshold Behavior for Steady-State Internal Transport Barriers in Burning Plasmas

J. García, G. Giruzzi, J. F. Artaud, V. Basiuk, J. Decker, F. Imbeaux, Y. Peysson, and M. Schneider

Association EURATOM-CEA, CEA/DSM/IRFM, Cadarache, F-13108 St. Paul lez Durance, France

(Received 17 January 2008; published 25 June 2008)

Burning tokamak plasmas with internal transport barriers are investigated by means of integrated modeling simulations. The barrier sustainment in steady state, differently from the barrier formation process, is found to be characterized by a critical behavior, and the critical number of the phase transition is determined. Beyond a power threshold, alignment of self-generated and noninductively driven currents occurs and steady state becomes possible. This concept is applied to simulate a steady-state scenario within the specifications of the International Thermonuclear Experimental Reactor.

DOI: 10.1103/PhysRevLett.100.255004 PACS numbers: 52.25.Fi, 52.35.Ra, 52.55.Hc

Steady-state regimes are the ultimate goal of magnetically confined fusion research. In tokamak devices, these regimes are based on the noninductive current drive concept [1], and their exploration will be a major objective of the next-step tokamak experiment, International Thermonuclear Experimental Reactor (ITER) [2]. A burning plasma confined by strong magnetic fields in the tokamak configuration is a complex physical system, particularly rich in intriguing physics properties if maintained in a steady state by high-power waves and/or high-energy particle injection. A new example of such properties, found by numerical simulation, is given in this Letter: the existence of a critical threshold in the injected power, beyond which a steady state becomes possible. This threshold has been characterized as a second-order phase transition with a critical number which is found to be similar to those of other completely different phenomena such as, e.g., the paramagnetic-ferromagnetic transition.

The complexity of the steady-state thermonuclear burn phase of a tokamak plasma stems from its intrinsic nonlinearity. The power source that sustains the burn is in large part produced by the plasma itself, via self-heating due to the energetic α particles produced by the fusion reactions (typically, 1/2–2/3 of the heating power in ITER, greater than 80% in a commercial reactor). The current flowing in the plasma and necessary for the stability of the magnetic configuration should also be self-generated, to a large extent (30%–70% in ITER, even more in a reactor). The mechanism providing this self-generation is called the bootstrap current [3]: this current is driven by the pressure gradient, in conjunction with trapping of charged particles in the magnetic field inhomogeneities. High bootstrap current fractions are more likely to be obtained in the presence of an internal transport barrier (ITB) [4,5], i.e., a sharp increase of the pressure gradient due to turbulence suppression. Finally, the remaining part of the plasma current, typically driven by radio frequency (rf) waves [1], is intrinsically associated with non-Maxwellian electron distribution functions, thus depends on the wave-plasma interaction properties, and can also give rise to nonlinear behavior [6]. Real-time control techniques can of course be used in order to master this complexity. However, the external heat and current sources available for such a control will always represent a minority with respect to the self-generated ones; therefore, naturally stable states have to be sought, around which control is possible.

In ITER, steady-state regimes correspond to very long pulses (3000 s), as required for significant neutron fluence and the associated tritium breeding module testing. This must be combined with a high enough fusion gain (defined as the ratio between the power produced by the fusion reactions and the additional heating power): $Q \geq 5$. In contrast with most present-day experiments, ITBs will be associated with negative magnetic shear s (i.e., to current density profiles that are hollow in the hottest part of the discharge) rather than with rotation shear, owing to the lack of a powerful torque source. This implies that the control of the current density profile is essential to sustain ITBs for a long time. Now, the bootstrap current naturally peaks where the pressure gradient is maximum, i.e., at the ITB, which in turn is due to a current that peaks outside the ITB itself. This is known as the current alignment problem, which may lead, in experiments [5] and even in simulations [7], to progressive shrinking and erosion of the ITB. Although various scenarios have been considered for steady-state operation on ITER [7,8], no steady sustainment of ITB for times of the order of 3000 s, with the power available expected on ITER ($P_{\mathrm{NBI}} < 33$ MW, $P_{\mathrm{IC}} < 20$ MW, $P_{\mathrm{EC}} < 20$ MW, $P_{\mathrm{LH}} < 20$ MW, for neutral beam, ion cyclotron, electron cyclotron, and lower hybrid powers, respectively) has been documented in simulations so far.

In this Letter, we present a conceptual solution to this problem, and use state-of-the-art integrated simulations to demonstrate its viability, within a framework of reasonable assumptions. It will be shown that this solution relies on specific properties of the ITB formation and the steady-state sustainment process, which behaves as a continuum phase transition [9], for which the most effective control parameter is identified as the local current source in the

vicinity of the ITB location. This localized current can be generated by electron cyclotron current drive (ECCD), with a well-defined power threshold. This provides, for the first time, a scenario for the steady-state phase of ITER, which satisfies the physics and operational constraints related to current alignment in the presence of an ITB.

These studies have been performed by means of the CRONOS suite of codes [10], which solves the transport equations for various plasma fluid quantities (current, energy, matter, momentum). This is done in one dimension (the magnetic flux coordinate associated with the minor radius), self-consistently with two-dimensional magnetic equilibrium. In particular, the fusion power is evaluated here by the orbit following Monte Carlo code SPOT [11]. The LH power deposition and driven current have been computed inside CRONOS by means of the LUKE/C3PO code [12], i.e., a 3D Fokker-Planck code coupled to toroidal ray tracing.

In order to study the ITB formation for ITER in reversed shear scenarios, a model for the reduction of turbulent transport in such regimes is needed. Since no first-principles model is able to simulate ITB formation in present-day tokamaks [13], the heat diffusivity model of the type used in Refs. [8,14] is used, i.e., $\chi_i = \chi_e = \chi_{i,\mathrm{neo}} + 0.4(1 + 3\rho^2)F(s)$, where ρ is the normalized radius coordinate, F is a shear function (vanishing for $s < 0$). This model has been extensively used to establish the ITER reference scenarios with ITB [8] and it is based on the experimental results obtained in the JT-60 upgrade tokamak [15] with ITB shots. It must be considered as a kind of minimal model which is used here to ensure that the phenomena we analyze do not depend on specific ingredients of models, but only on their common feature: the confinement improvement associated with $s < 0$. Since the pedestal main features cannot be predicted with enough accuracy [16], the pedestal temperature is fixed at $\rho \approx 0.93$ to $T_{\mathrm{ped}} \approx 3$ keV, which is a conservative value, with respect to the bootstrap current generated in the edge region. The electron density profile is prescribed with a ramp in the early phase of the regime, then fixed, and the global parameters for the ITER steady-state reference scenario 4 have been considered [7], except the total current, which has been downscaled to 8 MA.

To avoid shrinking or erosion of the ITB, a method is needed to control the dominant current component, i.e., the bootstrap current, which is in turn essentially related to the dominant heating source, i.e., the α heating. For such a purpose, a pure rf scenario without neutral beam current drive (NBCD) has been considered, which is obtained using $P_{\mathrm{IC}} \approx 20$ MW (53 MHz, 2nd tritium harmonic), $P_{\mathrm{EC}} \approx 21$ MW (170 GHz, O mode), $P_{\mathrm{LH}} \approx 13$ MW (5 GHz, parallel refractive index $n_{\parallel} = 2$). The 21 MW of EC power are deposited at $\rho \approx 0.45$ by using 13 MW from the upper steering mirrors of the top launcher at toroidal injection angle $\varphi_{\mathrm{tor}} = 20°$ and poloidal injection angle $\varphi_{\mathrm{pol}} = 67°$ and 8 MW from the upper row of the equatorial launcher at $\varphi_{\mathrm{tor}} = 20°$ and $\varphi_{\mathrm{pol}} = 67°$ [17]. The plasma density, the electron and ion temperature profiles, as well as the current density profiles obtained at $t = 3000$ s and the evolution of the q profile from $t = 2000$ s are shown in Fig. 1. The current density profile obtained shows a maximum at $\rho = 0.45$, which is at the same time at the maximum of the bootstrap current and of the ECCD. Therefore, the ECCD locks the ITB at midradius and avoids its erosion and shrinking; however, there is a clear power threshold for this feature as will be shown in the following. The LH power deposition is located at $\rho = 0.7$, and the current drive obtained ($\approx$0.6 MA) contributes to the total noninductive current fraction ($f_{\mathrm{ni}} \approx 97\%$). A small amount of central current drive (e.g., by fast waves, $I_{\mathrm{fwcd}} = 20$ kA) is added in order to control q_0. This current prevents excessive increase of q_0, which would imply loss of α particle confinement [11]. With this current drive scheme, the q profile obtained is stable for 1000 s, as shown in Fig. 1, with $q_0 \approx 6$ and $q_{\mathrm{min}} > 2$. The reversed q allows a reduction of anomalous transport close to the ion neoclassical level, which finally leads to a temperature profile rather flat in the plasma core, and a large normalized temperature gradient, $R/L_{\mathrm{Te}} = 27$ (where R is the plasma major radius and $L_{\mathrm{Te}} = |\nabla T_e/T_e|^{-1}$ with T_e the electron temperature), at $\rho = 0.45$ as shown in Fig. 1. With these

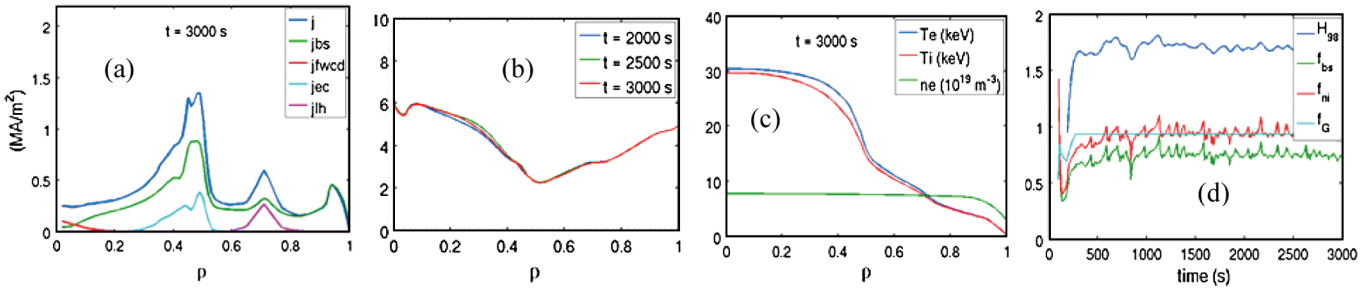

FIG. 1 (color). Total current (j), bootstrap current (jbs), fast wave (jfwcd), electron cyclotron (jec), and lower hybrid (jlh) current drive density profiles at $t = 3000$ s (a). Evolution of the q profile (b). Electron, ion temperature, and density profiles at $t = 3000$ s (c). Time evolution of H_{98}, f_{bs}, f_{ni}, and f_G (d).

results the fusion power is 70 MW with a fusion gain $Q = 6.5$. The time evolution of the confinement enhancement factor with respect to the standard ITER scaling law [2], H_{98}, the bootstrap current fraction, the Greenwald fraction, and the total noninductive current fraction are shown in Fig. 1(d). The bootstrap current fraction ($f_{bs} = 70\%$) is stable during all the simulation and represents the main contribution to the total noninductive current. The plasma is above the no-wall stability limit ($\beta_N > 4li$), owing to the flatness of the current density profile; however, this feature is intrinsic to scenarios with ITB based on negative magnetic shear. The resulting H_{98} factor (=1.7) is relatively high: such an improvement over the ITER reference scenario is needed in order to obtain the amount of bootstrap current required for steady-state operation.

The role played by the ECCD system is essential for this regime, since it is not only used in the ramp-up phase with the aim of creating the ITB, but it is also critical to sustain the ITB for a long time. In Fig. 2(a), the dependence of R/L_{Te} on the EC power (normalized to the average density) is shown. The red curve corresponds to the short time scale response to ECCD, i.e., 100 s after its application (of the order of 1 resistive time), whereas the blue curve yields the steady-state result ($t = 3000$ s). It appears that the two responses are governed by different physics: there is a clear jump in the steady-state response at $P_{EC}/\langle n_e\rangle \approx 1.3 \times 10^{-19}\,\mathrm{MW\,m^{-3}}$ for the $t = 3000$ s curve, above which an ITB is obtained with much higher R/L_{Te} for small variations of $P_{ECH}/\langle n_e\rangle$. In fact, this threshold clearly splits the regime obtained in one close to the inductive scenarios for $P_{EC}/\langle n_e\rangle < 1.3 \times 10^{-19}\,\mathrm{MW\,m^{-3}}$, ($H_{98} = 1.1$, $f_{bs} = 37\%$, $R/L_{Te} = 12.5$) and another one with steady-state for $P_{EC}/\langle n_e\rangle \gg 1.3 \times 10^{-19}\,\mathrm{MW\,m^{-3}}$ ($H_{98} = 1.7$, $f_{bs} = 70\%$, $R/L_{Te} = 27$). It is worth pointing out that this threshold on the EC power is obtained for the global process of creation and sustainment of the ITB, in contrast with the short time scale response, which shows no threshold for the power range considered, as observed in experiments whenever the time might not be long enough [18]. Although obtained for a particular transport model, the behavior presented in Fig. 2(a), which constitutes the main result of this work, is largely independent of the details of the transport model: it is basically associated with the dynamics of resistive current diffusion in the presence of localized current sources.

The threshold obtained for the EC power is reminiscent of similar critical behaviors that appear in the ITB formation of other completely different fusion devices as, e.g., the Large Helical Device (LHD) [19], which has been characterized as a second-order phase transition [20]. In this case, the R/L_{Te} parameter can be taken as the order measure of the system and $P_{EC}/\langle n_e\rangle$ as the control parameter (for this fixed EC wave launching geometry). Since the ITB is obtained by means of negative magnetic shear, which continuously changes according to current diffusion, the order parameter is also continuous at the transition point, and therefore this process also corresponds to a second-order phase transition, as it has been pointed out previously according to experimental evidence [21] in JET. In fact, the blue curve of Fig. 2(a) can be properly fitted as

$$R/L_{Te} - 12.5 \begin{cases} \approx 0 & P_{EC}/\langle n_e\rangle < 1.3 \times 10^{-19}\ \mathrm{MW\,m^{-3}} \\ \propto [P_{EC}/\langle n_e\rangle]^{\beta} & P_{EC}/\langle n_e\rangle > 1.3 \times 10^{-19}\ \mathrm{MW\,m^{-3}}, \end{cases} \quad (1)$$

with $\beta = 0.60$ and fit correlation coefficient $r = 0.996$. Although the β parameter is somewhat higher than the one obtained in the case of LHD [20], it is still close to the typical values obtained for second-order phase transitions and, in particular, in the case of the mean field model, $\beta = 0.5$ [9].

An important point is that the threshold obtained is a consequence of the minimum EC-driven current (not just the EC heating) needed in order to maintain the ITB. In fact, as shown in Fig. 2(b), if the ECCD is removed after 2000 s but the EC heating is maintained, the ITB starts to shrink and finally a typical inductive current density profile

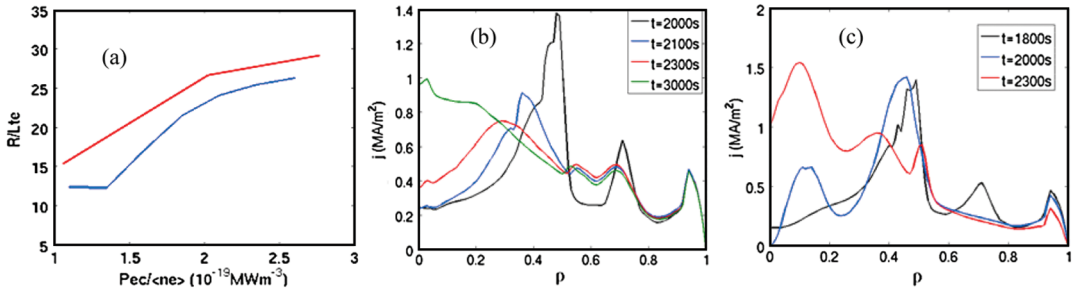

FIG. 2 (color). R/L_{Te} at the ITB location versus $P_{EC}/\langle n_e\rangle$ at $t = 3000$ s (blue, steady-state behavior) and at 200 s (red, transient behavior) (a). Evolution of the current profile after the ECCD is removed at $t = 2000$ s (b). Evolution of the current density profile after the addition of 12 MW of NBI heating by removing 12 MW of ICRH and the LH system at $t = 1800$ (c).

is obtained. This behavior has been found experimentally in DIII-D tokamak fully noninductive scenarios [22], and in fact the problem of erosion and shrinking of ITB has usually been a major issue on ITER steady-state scenario simulations [7]. Moreover, the threshold obtained, and its dependence on the ECCD, are directly related to the fact that a minimum negative magnetic shear is needed to sustain the ITB. According to the models applied in this Letter, even a slightly negative magnetic shear is sufficient to trigger the ITB, but it is not enough to sustain it, and a minimum value, $s = -0.8$, is found to be necessary during all the simulation. This fact clearly shows the necessity of having enough current drive power with well localized deposition in ITER to provide such a minimum negative magnetic shear.

The role played by the noninductive currents inside and outside the ITB is quite different. In fact, the LH current drive and the bootstrap current at the edge contribute to the total noninductive current without affecting the ITB, in contrast with current sources inside the ITB. This is shown in Fig. 2(c), where 12 MW of NBCD have been added, 12 MW of ion cyclotron resonance heating (ICRH) have been removed, and the lower hybrid current drive has been also removed in order to keep constant the global heating and current driven in the plasma at 1800 s. The current diffusion due to the high amount of current added inside the ITB ($=0.7$ MA) makes the q profile drop in that region, which finally leads to the erosion of the ITB, as also obtained in other studies [7], since the magnetic shear is below the threshold. After the ITB is lost, the total current keeps growing in the center, and finally $q_0 < 1$.

In conclusion, a critical behavior has been found for the global process of ITB formation and sustainment in tokamaks by means of the suppression of turbulent transport due to negative magnetic shear. The main feature of this scenario is that a minimum negative magnetic shear is required to steadily sustain the ITB, a much stronger requirement than that needed for the ITB formation. This critical system has been characterized as a second-order phase transition, with the normalized temperature gradient as the order parameter and $P_{\mathrm{EC}}/\langle n_e \rangle$ as the control parameter (since it controls the magnetic shear in the plasma). The critical number obtained is comparable to other completely different physical systems (and close to that obtained in the mean field theory for these transitions [9]) and to that found for the LHD stellarator [20]. Therefore, in spite of the fact that different physical mechanisms can be involved in the ITB formation and sustainment in stellarators and tokamaks (rotation in [20], negative magnetic shear here), both can belong to the same universality class as other critical physical systems.

The critical behavior found in this Letter has significant consequences for ITER. Since the critical shear obtained is strongly negative, $s = -0.8$, large current drive inside the ITB (e.g., NBCD) destroys it after some current diffusion times due to misalignment of the currents. However, the new scenario proposed here for ITER steady-state plasmas with only radio frequency heating systems provides a solution to the well-known problem of current alignment, which caused the shrinking and erosion of the ITB in previous studies performed with NBCD. The present design of the EC power system in ITER can provide such a negative magnetic shear at $\rho = 0.45$ through ECCD. Nevertheless, the definition of a viable steady-state scenario for ITER still has to overcome several problematic issues. Impurity confinement and particle fueling inside the ITB, specific MHD related to the inverted q profile (resistive interchange modes, double tearing, infernal modes), and Alfvén instabilities driven by the α particles are the most difficult challenges, requiring extensive theoretical, computational, and experimental efforts both before and during the first phases of the ITER operation.

Fruitful discussions in the framework of the International Tokamak Physics Activity/Steady-state Operation Group are gratefully acknowledged

[1] N. J. Fisch, Rev. Mod. Phys. **59**, 175 (1987).
[2] M. Shimada *et al.*, Nucl. Fusion **47**, S18 (2007).
[3] R. Bickerton, J. W. Connor, and J. B. Taylor, Nature (London) **229**, 110 (1971).
[4] J. W. Connor *et al.*, Nucl. Fusion **44**, R1 (2004).
[5] X. Litaudon, Plasma Phys. Controlled Fusion **48**, A1 (2006).
[6] G. Giruzzi *et al.*, Phys. Rev. Lett. **91**, 135001 (2003).
[7] W. A. Houlberg *et al.*, Nucl. Fusion **45**, 1309 (2005).
[8] A. R. Polevoi *et al.*, in *Proceedings of the 19th IAEA Fusion Energy Conference, Lyon, 2002* (IAEA, Vienna, 2003), file CT/P-08.
[9] E. M. Lifshitz and L. P. Pitaevskii, *Statistical Physics* (Pergamon, New York, 1980).
[10] V. Basiuk *et al.*, Nucl. Fusion **43**, 822 (2003).
[11] M. Schneider *et al.*, Plasma Phys. Controlled Fusion **47**, 2087 (2005).
[12] Y. Peysson and J. Decker, in *Proceedings of the 34th EPS Conference on Controlled Fusion and Plasma Phyics, Warsaw, 2007* (EPS, Paris, 2007).
[13] T. Tala *et al.*, Nucl. Fusion **46**, 548 (2006).
[14] F. Albajar *et al.*, Nucl. Fusion **45**, 642 (2005).
[15] T. Fujita *et al.*, Phys. Rev. Lett. **78**, 2377 (1997).
[16] M. Sugihara *et al.*, Plasma Phys. Controlled Fusion **45**, L55 (2003).
[17] G. Ramponi *et al.*, Fusion Sci. Technol. **52**, 193 (2007).
[18] K. Ida *et al.*, Plasma Phys. Controlled Fusion **46**, A45 (2004).
[19] M. Yokoyama *et al.*, Nucl. Fusion **47**, 1213 (2007).
[20] J. Garcia *et al.*, Phys. Rev. Lett. **96**, 105007 (2006).
[21] P. Mantica *et al.*, Phys. Rev. Lett. **96**, 095002 (2006).
[22] M. Murakami *et al.*, Phys. Rev. Lett. **90**, 255001 (2003).